Room Temperature Large and Reversible Modulation of Photoluminescence by In-situ Electric Field in Ergodic Relaxor Ferroelectrics

Hailing Sun, Xiao Wu, Deng Feng Peng, K.W. Kwok*

Department of Applied Physics, The Hong Kong Polytechnic University, Kowloon, Hong Kong, China

ABSTRACT: Ferroelectric oxides with luminescent ions hold great promise in future optoelectronic devices because of their unique photoluminescence and inherent ferroelectric properties. Intriguingly, the photoluminescence performance of ferroelectric ceramics could be modulated by an external electric field. However, researchers face a current challenge of the diminutive extent and degree of reversibility of the field-driven modification that hinder their use in room temperature practical applications. Within the scope of current contribution in rare-earth doped bismuth sodium titanate relaxors, the most important information to be noted is the shifting of the depolarization temperature towards room temperature and the resulting considerable enhancement in ergodicity, as evidenced by the dielectric properties, polarization and strain hysteresis, as well as the in-situ Raman/ X-ray diffraction studies. After the introduction of 1 mol% Eu, the induced composition and charge disorders disrupt the original long-range ferroelectric macro-domains into randomly dynamic and weakly correlated polar nanoregions, which facilitates a reversible transformation between polar nanoregions and unstable ferroelectric state under an electric field, engendering a large strain. By virtue of this, both the extent and degree of

reversibility of photoluminescence modulation are enhanced (~ 60%) considerably, and room-temperature in-situ tunable photoluminescence response is then achieved under electric field. These should be helpful for the realization of regulating the physical couplings (photoluminescent-ferroelectrics) in multifunctional inorganic ferroelectrics with a high ergodic state by reversibly tuning the structural symmetry.

1. INTRODUCTION

Spectroscopic tuning and rapidly reversible manipulation of photoluminescence (PL) activities are highly essential not only for exploring the underlying physical processes but also for widespread applications, such as long-distance quantum communication, photonic devices, volumetric 3D display, back light, and biomedicine.[1-6] It is cogent that the crystalline symmetry changes induced by phase transition, polarization, and strain bridge a relationship between the way of an external electric field modification and the corresponding photoluminescence behavior.[4,7-9] In our previous work, we demonstrated a real-time electric field-induced PL modulation in Pr-doped $Ba_{0.85}Ca_{0.15}Ti_{0.90}Zr_{0.10}O_3$ ferroelectric ceramic by virtue of its obviously ferroelectric phase transformation accompanied with polarization switching.[10] However, the physical mechanism and the interplay process between electric field and PL emissions in inorganic materials have remained to be fully elucidated because of their notably complicated and mutative crystal structures under electric field. Moreover, for practical applications, it is requisite to enhance both the extent and degree of reversibility of the electric field-driven modulation at room temperature. Among the lead-free ceramic systems, the bismuth sodium titanate (BNT)-based one has drawn considerable attention, since the Bi^{3+} ion owns the second-highest polarizability (after Pb^{2+}) caused by the $6s^2$ lone pairs that could contribute to a large structural distortion and extraordinarily large strain under electric field.[11-13] Similar to other relaxors, it undergoes a transition from an ergodic relaxor state

to a non-ergodic relaxor state as the temperature decreases and passes through the ferroelectric-relaxor transition temperature T_{F-R}. Non-ergodic relaxors will transform into a long-range ordered ferroelectric state irreversibly under a sufficiently strong electric field while the transformation for ergodic relaxors is reversible attributing to the strong internal random fields.[14-18] 0.94BNT-6BaTiO$_3$ (BNT6BT) is a solid solution of BNT and BT with composition near the morphotropic phase boundary. It is an non-ergodic relaxor at room temperature, capable of exhibiting an ordered ferroelectric state as evidenced by the butterfly-shaped strain hysteresis [8,15] and good piezoelectric properties.[19] At temperatures above T_{F-R} (~75°C), it features a large (reversible) strain owing to the thermally induced ergodicity, i.e., the increase in random fields and vanishing of ferroelectric state arisen from thermal effects.[16,20-21] Via chemical modifications (e.g., formation of solid solutions with $K_{0.5}Na_{0.5}NbO_3$ [22] or $(Bi_{1/2}K_{1/2})TiO_3$-$SrTiO_3$ [23]) or doping with various lanthanide elements (such as Pr, Eu) [8,24] for mimicking the thermal effects, T_{F-R} can be lowered to near room temperature. Yao Q. et al. have shown that the T_{F-R} of BNT-BT ceramics can be lowered from 76°C to ~ 25°C by the doping of 0.8 mol% Pr.[8] Practically, T_{F-R} is often related to the depolarization temperature T_d that is defined as the temperature at which the aligned polarization (with long-range order) vanishes because of thermal effect.

Recently, it has been reported that a BNT6BT ceramic doped with 0.5% Eu exhibits a distinct irreversible change in PL emissions after poling (i.e., ex-situ mode) at room temperature. The (same) change becomes reversible when the ceramic is subject to an external electric field (i.e., in-situ mode) at elevated temperature ~80°C, which is above T_{F-R} or close to the depolarization temperature (T_d ~85°C) of the ceramic. On the basis of these results, we anticipate that a reversible change in PL can be realized at room temperature by lowering the T_{F-R} or T_d of the ceramics via, for example, increasing the doping level of Eu. However, PL emissions will become weakened at

high doping levels of rare earth elements because of the concentration-quenching effect.[25,26] For BNT-BT ceramics, it occurs normally at a doping level of 0.8 mol%.[25] In balancing the reversibility and intensity, the present work thus aims at realizing a real-time electric field-induced PL modulation at room temperature in a BNT6BT ceramic doped with 1 mol% Eu (Eu-BNT6BT) as well as elucidating the underlying mechanism in correlation with structural distortion and macroscopic strain. As compared with our previous work on Pr-doped BCTZ ceramics, both the extent and degree of reversibility of the PL modulation are largely enhanced (~40%). Moreover, the PL modulation is not governed by the ferroelectric phase transition or polarization switching. It is anticipated that via doping a high concentration of Eu (1 mol%), the cation disorder at the mixed A-sites of BNT6BT becomes larger and more A-O bonds are broken. A mixture containing more nano-domains (polar nanoregions, PNRs) is thus produced, favoring the transition to ergodic relaxor state via lowering T_{F-R} to near room temperature.[16,27]

2. EXPERIMENTAL SECTION

2.1. Samples Fabrication. $0.94Bi_{0.5}Na_{0.5}TiO_3$-$0.06BaTiO_3$ ceramics doped with 1 mol% Eu^{3+}, abbreviated as Eu-BNT6BT, were prepared by a conventional solid-state method using high-purity metal oxides or carbonate powders: Na_2CO_3 (99%), Bi_2O_3 (99.9%), TiO_2 (99.9%), $BaCO_3$ (99.5%), and Eu_2O_3 (99.9%). The powders in the stoichiometric ratio were ball-milled thoroughly in anhydrous ethanol using zirconia balls for 12 h, then calcined at 900 °C for 2h in air before ball-milled again for 12 h and sieved through an 80-mesh screen. After mixed thoroughly with a binder of polyvinyl alcohol solution (5 wt%), the resulting mixture was pressed into disk samples. Then, the samples were finally sintered at 1170°C for 3h in air for densification. The ceramics were poled under an electric field of 7 kV/mm at room temperature in silicone oil for 30 min. Similar to our previous work, a sandwiched structure is used for continuously detecting the in-situ Raman, X-ray

diffraction (XRD) and photoluminescence (PL) properties of the samples. A silver electrode (~10 μm thick) was first coated on the back surface of a thin ceramic disk (~150 μm thick), then a conductively transparent electrode of indium tin oxide (ITO) (~0.4 μm thick) was deposited on the top surface at 250°C by magnetron sputtering. Both the silver and ITO electrodes are of the same diameter (~10 mm) of the sample. The transparent ITO enables the excitation and emission light to pass through under an external electric field applied along the thickness direction.

2.2. Measurements. The crystallite structure was examined using XRD analysis with CuK$_\alpha$ radiation (SmartLab, Rigaku Co., Japan). The dielectric constant (ε_r) and dielectric loss (tan δ) were measured as functions of temperature using an impedance analyzer (HP 4194A, Agilent Technologies Inc., Palo Alto, CA). The Raman spectra were recorded using a Raman system from Princeton Instruments (HORIBA HR800). The piezoelectric coefficient (d_{33}) was measured using a piezo-d_{33} meter (ZJ-3A, China). The ferroelectric properties and strain performance were acquired using a TF2000 analyzer (Aixacct, Aachen, Germany). The PL visible emission spectra were measured by a spectrophotometer (FLSP920, Edinburgh Instruments, UK) using a 450-nm xenon arc lamp (Xe900) as the excitation source. A voltage source (2410 1100V Source meter, Keithley Instruments Inc., US) was used to apply external voltage for investigating the E-field dependent in-situ Raman, XRD and PL properties.
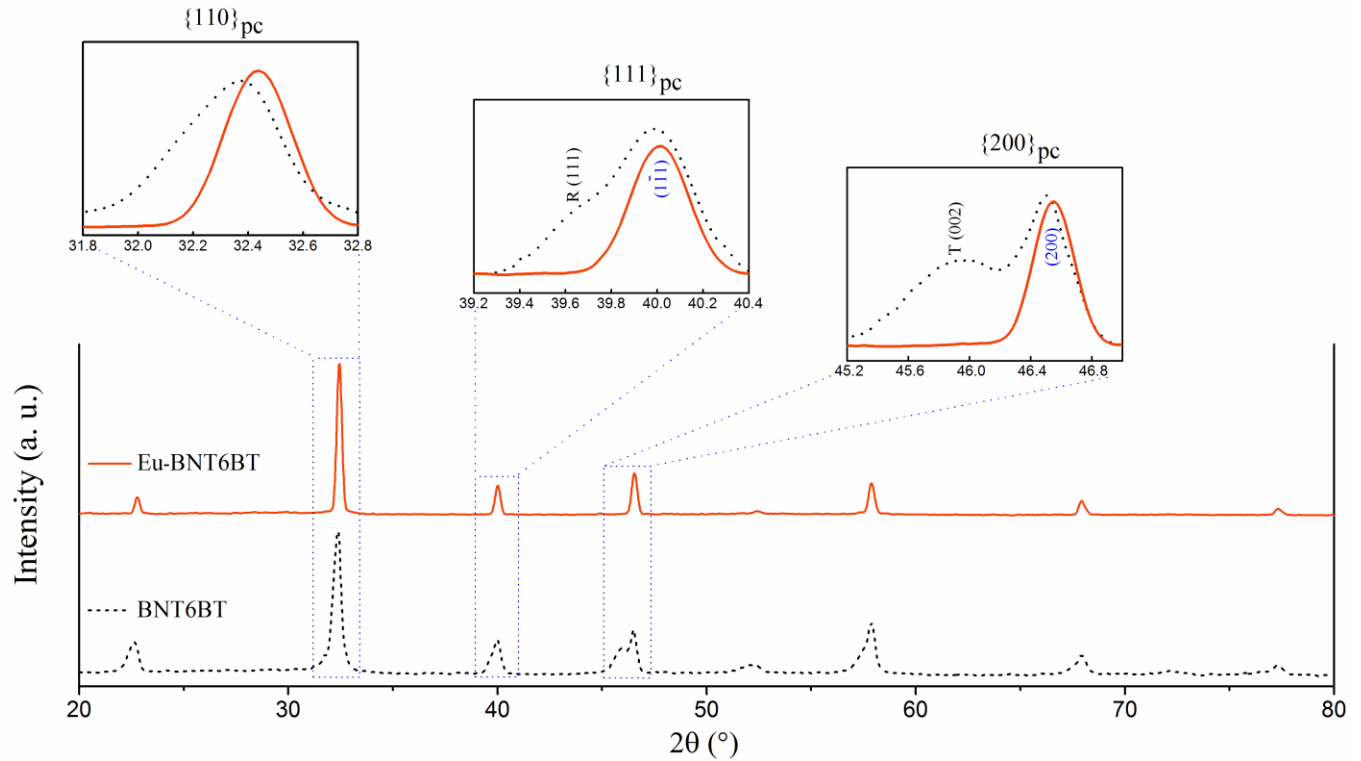
3. RESULTS AND DISCUSSION

Figure 1 General XRD patterns comparison of BNT6BT (dot) and Eu-BNT6BT (line) relaxors. The insets show a fine scanning of three characteristic diffraction peaks labeled as {110}pc, {111}pc and {200}pc, respectively.

3.1. Structure Identification and Ergodic Relaxor. Structural analysis was first conducted

based on the XRD patterns of the as-prepared BNT6BT and Eu-BNT6BT ceramics. As shown in

Figure 1, both the ceramics possess a perovskite structure at room temperature. No additional

peaks reflecting the presence of rare-earth oxides are observed within the resolution limit for the

Eu-BNT6BT ceramic, suggesting that Eu^{3+} has diffused into the BNT6BT host lattice. The insets

of Figure 1 show the close inspection of three characteristic diffraction peaks labeled as {110}pc,

{111}pc and {200}pc, respectively. In agreement with the previous findings of the coexistence of

rhombohedral (R) and tetragonal (T) phases,[28-31] the BNT6BT ceramic exhibits split diffraction

peaks of R(111)/(1$\bar{1}$1) and T(002)/(200) at 2θ ~ 40° and ~46°, respectively and a relatively broad

{110}c diffraction peak at 2θ ~33°. In contrast, all those diffraction peaks of the Eu-BNT6BT

ceramic become relatively sharp and center-symmetric, and no splitting is observed. Apparently,

it possesses a cubic-like or pseudo-cubic symmetry.[7,27,28,32] Nevertheless, it is suggested to contain mainly PNRs of R3c and P4bm embedded in a pseudocubic matrix, each of the PNRs is slightly distorted from cubic. It has been shown by transmission electron microscopy and neutron diffraction studies that the rhombohedral and tetragonal phases of BNT6BT belong to the R3c and P4bm space groups, respectively, and part of them are presented as nano-scale entities with polar displacements called PNRs.[17,33-34] Owing to the similar ionic radii of Na^+ (1.39 Å, CN=12) and Bi^{3+} (1.36 Å, CN=12), the substitution with Eu^{3+} (1.26 Å, CN=12) would increase compositional disorder as well as heterovalent ions, and thus leading to the formation of more discrete nano-domains (i.e., PNRs) via the disruption of the original ferroelectric macro-domains.[35] However, as limited by the resolving capability of our regular X-ray diffractometer, the symmetries of the nano-scale entities cannot be detected accurately (because of peak broadening)[36-37] and appear cubic-like or pseudo-cubic with diffraction peaks overlapping with those of the pseudocubic matrix. On the other hand, the substitution would induce a slight shrinkage of the lattices, and thus leading to a shift of the XRD peaks to larger angles as shown in Figure 1. It would also cause the lattice constants become similar with each other. Indeed, further investigation using advanced techniques such as transmission electron microscopy and neutron diffraction analysis are needed for understanding the exact crystal structures of the ceramic.

For confirming the increase in PNRs which give rise to all the unique relaxor characteristics, the temperature-dependent dielectric constant (ε_r) and dielectric loss (tan δ) of the as-prepared (un-poled) and poled Eu-BNT6BT ceramics have been measured, giving the results shown in Figure 2a and 2b, respectively. Both the samples exhibit two distinctive anomalies in the $\varepsilon_r(T)$ curves, i.e., a shoulder at a lower temperature (100°C) and a peak at a higher temperature (270°C). Both the shoulder and peak are diffusive and strongly frequency-dispersive,
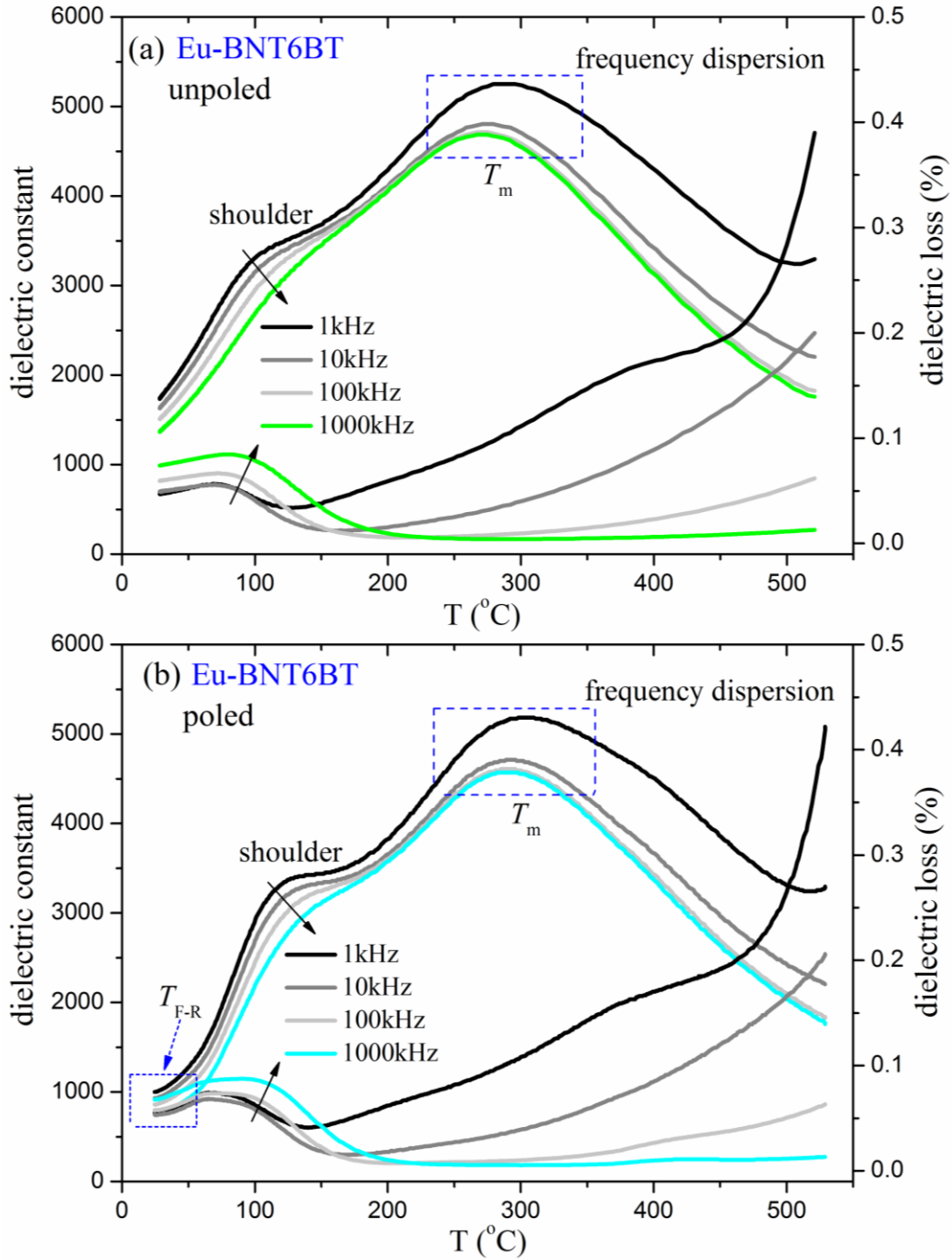
Figure 2 Temperature-dependent dielectric constant (ε_r) and dielectric loss (tan δ) of the (a) unpoled and (b) poled Eu-BNT6BT relaxor.

demonstrating the unique characteristic of relaxor ferroelectrics.[23,26,38] Together with the enhanced

frequency dispersion of the high-temperature anomaly as compared with the (un- poled) BNT6BT

ceramic (Figure S1), it is clear that the Eu-BNT6BT ceramic contains a considerable and even larger amount of PNRs. It has been shown for BNT6BT that the low-temperature anomaly is attributed to thermal evolution of the relaxation time distribution of the coexisting R3c and P4bm PNRs. Upon further heating, the PNRs of R3c symmetry transform into P4bm, and then all of them undergo another thermal evolution, altogether giving rise to the high-temperature anomaly.[23,38] Our results hence suggest that the substitution with Eu has effectively disrupted the original ferroelectric domains for forming more PNRs. The compositional disorder as well as heterovalent ions disturbance arisen from the Eu-substitution may also destabilize the PNRs to become more dynamic and weakly correlated with each other, and hence lowering T_{F-R} (or T_d) to below room temperature.[18] It is evidenced by the absence of an abrupt change in ε_r or a noticeable peak in tan δ near the low-temperature shoulder for the poled sample (Figure 2b). Under a strong electric field (at room temperature), the local random fields exerted by PNRs are overcome, and the dynamic PNRs are aligned and then transform into ordered ferroelectric domains. For non-ergodic relaxors such as BNT6BT, the ordered ferroelectric domains are preserved after the removal of the electric field, engendering macroscopically measureable piezoelectric properties (as exemplified by the large piezoelectric coefficient of 155 pC/N for BNT6BT). Evidently, the ordered ferroelectric domains will be smashed upon heating and the randomly oriented PNRs will be restored, manifesting as an abrupt change and/or a peak in the temperature plots of ε_r and tan δ, respectively (Figure S1). Accordingly, as demonstrated in Figure 2b, the Eu-BNT6BT ceramic should be in the ergodic relaxor state at room temperature and discrete PNRs with random orientations are reinstated after the poling process (the application and removal of a strong electric field).[16,18]
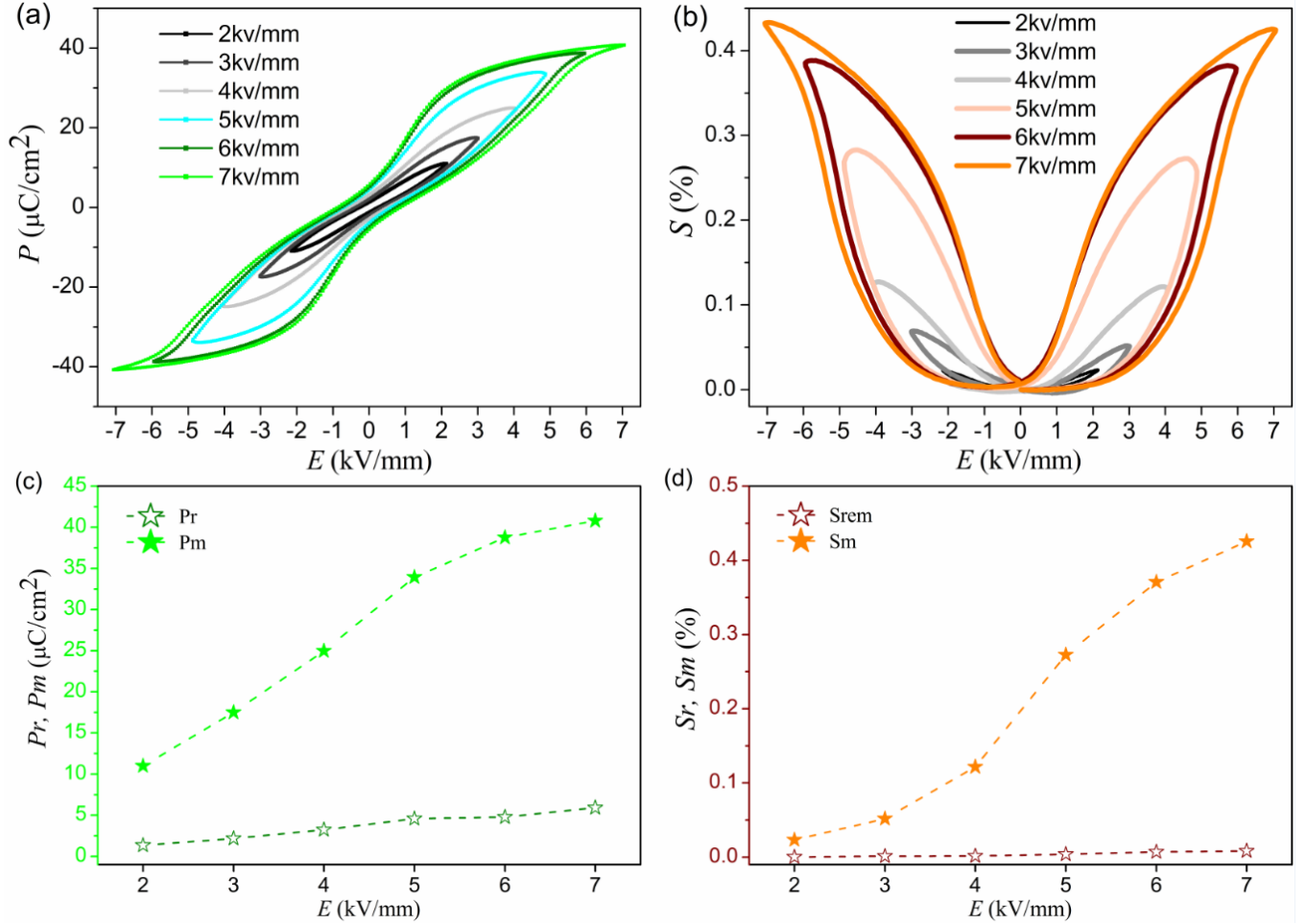
Figure 3 (a) The polarization hysteresis (P-E) and (b) bipolar strain hysteresis (S-E) loops of the Eu-BNT6BT relaxor, respectively; (c-d) the corresponding maximum polarization (P_m), remanent polarization (P_r), as well as maximum strain (S_m) and remanent strain (S_r) dependencies on E field.

3.2. Ergodicity and Reversible Large Strain. The polarization hysteresis (P-E) and bipolar strain hysteresis (S-E) loops of the Eu-BNT6BT ceramic are shown in Figure 3a and 3b, respectively. Slim and constricted P-E loops are obtained under ac electric fields with magnitude higher than 4 kV/mm (Figure 3a). This clearly demonstrates that the ceramic possesses polar/non-cubic ferroelectric phases and the ordered ferroelectric domains developed under high electric fields cannot be preserved at zero field. This also provides evidence to the ergodic relaxor state of the ceramic (at room temperature). The strong electric field induces a transformation of the

10

randomly oriented PNRs to ordered ferroelectric domains, contributing to the observed maximum polarization (P_m). Upon decreasing the electric field, the ferroelectric domains are smashed into discrete and randomly oriented PNRs because of the cooperative interactions, and thus causing the observed polarization to decrease and reach a low remanent polarization (P_r) at zero field. As shown in Figure 3c, the observed P_m increases continuously to 41 μC/cm^2 with increasing magnitude of the ac electric field, while P_r remains at a value smaller than 6 μC/cm^2, which is attested by a low piezoelectric coefficient of 16 pC/N.

As evidenced by the sprout-shaped S-E loops shown in Figure 3b, the electric field-induced transformations between PNRs and ferroelectric domains produce also a large and reversible strain. It can be seen from Figure 3d that the maximum strain (S_m) increases steadily to 0.43% as the magnitude of the ac electric field increases to 7 kV/mm, which is comparable to other BNT6BT-based relaxors at elevated temperatures.[20,24,39,40] The large strain may also be contributed by the transitions between PNRs with different symmetries (i.e., from P4bm to R3C under high electric fields) facilitated by their comparable free energies.[18,20,21] Similar to the remanent polarization, the remanent strain (S_r) remains at a value smaller than 0.008%, clearly demonstrating the reversibility of the electric field-induced strain as well as the alignments and/or transitions of PNRs.

3.3. Cycling Structural Changes with Ergodicity Feature. Owing to the high sensitivity to local ionic configurations, Raman spectroscopy has been widely used to study the symmetry changes such as oxygen octahedral tilting of relaxor ferroelectrics that comprise plenty of PNRs.[29,41] Accordingly, the in-situ Raman spectra of BNT6BT (Figure 4a) and Eu-BNT6BT (Figure 4b) ceramics have been measured under an electric field in the range of 0 to 7 kV/mm for studying their degree of ergodicity and reversibility. As shown in Figure 4, both the ceramics
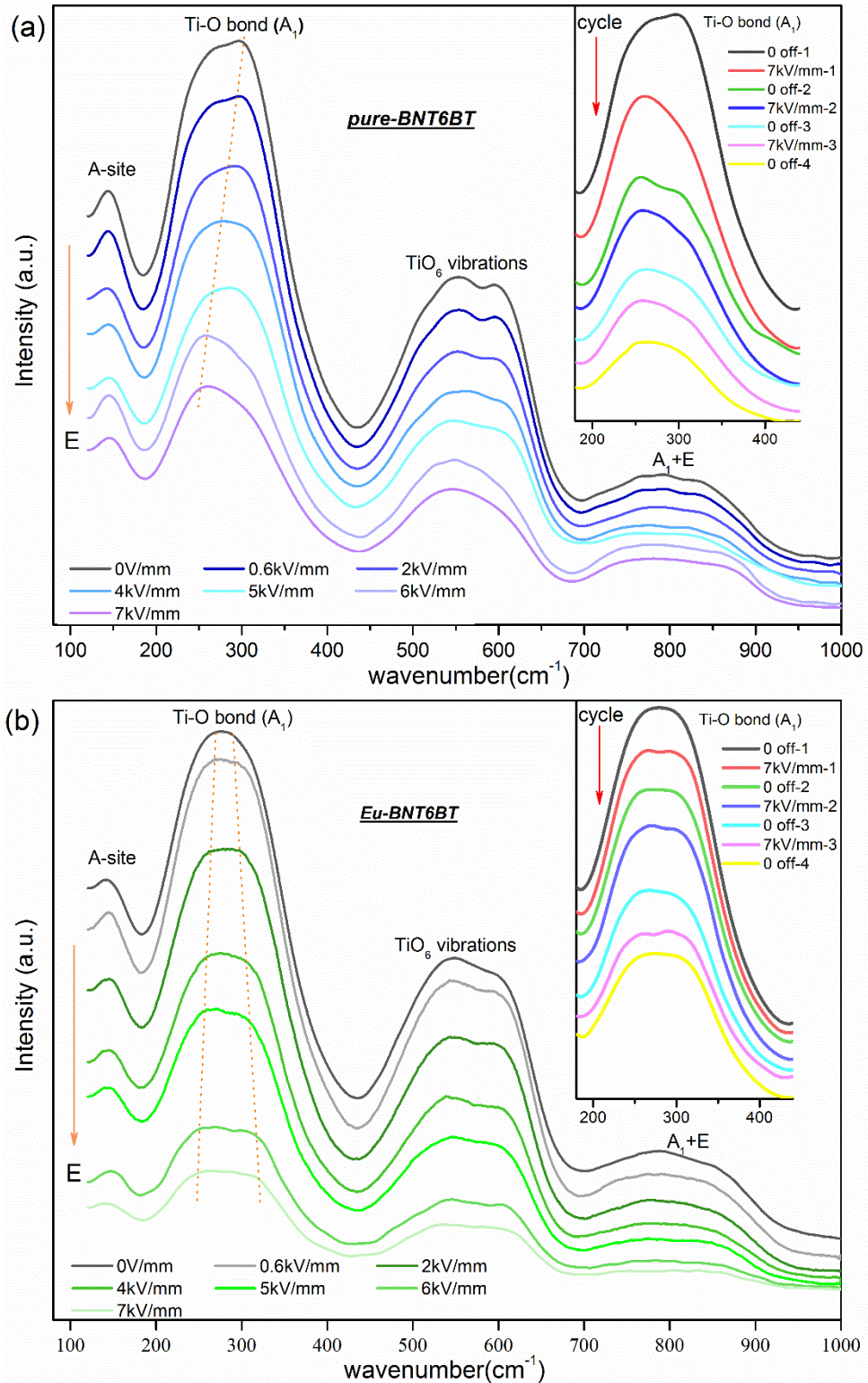
Figure 4 In-situ Raman spectra of (a) BNT6BT and (b) Eu-BNT6BT ceramics under an E field increasing from 0 to 7 kV/mm; with applying the off- and on-fields three times for the typical Ti-O Raman modes shown in the insets, respectively.

exhibit four Raman bands that are commonly observed for BNT-based ceramics. The band located at ~140 cm^{-1} is attributed to the stretching vibration of Na-O and Bi-O bonds, whereas the Ti-O stretching vibration contributes to the band at ~280 cm^{-1}. The rotation and vibration of the TiO6 octahedra give rise to the broad band in 450-650 cm^{-1} and the high-frequency bands above 700 cm^{-1} are associated with the overlapping of A$_1$ (longitudinal optical) and E (longitudinal optical) modes.[28,39,42-44] In general, all the bands of both ceramics are relatively broad, ascribing to the typical relaxor features of mode overlapping. As compared with BNT6BT, the Eu-BNT6BT ceramic exhibits a slightly larger bandwidth for all bands, attesting the enhancement in compositional disorder arisen from the substitution of Eu (Figure S2). Moreover, the broad Ti-O band corroborates the coexistence of the rhombohedral and tetragonal phases particularly in the Eu-BNT6BT ceramic where a slightly decrease in the tetragonal phase is also observed. It has been shown that the Ti-O band can be de-convoluted into A1(2) and B1 modes which are strongly related to the vibrations in rhombohedral and tetragonal phases, respectively.[41,45]

As also shown in Figures 4a-b, the ceramics exhibit different evolutions of the Ti-O band under electric fields. For the BNT6BT ceramic, the "peak" value of the band changes from ~300 cm^{-1} (contributed by B1 mode) to 260 cm^{-1} (contributed by A1(2) mode) as the electric field increases from 0 to 7 kV/mm. This indicates that (part of) the tetragonal phase has transformed into rhombohedral phase, and the ceramic becomes comprising predominantly rhombohedral phase. Similar electric field-induced phase transition has been demonstrated based on in-situ electric field X-ray diffraction and transmission electron microscopy studies.[33,46] In contrast, the bandwidth for the Eu-BNT6BT ceramic increases slightly with increasing electric field, and no significant change in relative intensities of the two modes (A1(2) and B1) is observed. This suggests that the rhombohedral and tetragonal phases still coexist in the ceramic. However, the

electric field-induced tetragonal-to-rhombohedral phase transition commonly observed in the BNT6BT ceramic[39,44,47,48] cannot be excluded. The increase in bandwidth, on the other hand, may be related to the alignment and then deformation of the PNRs induced by the electric field.

The reversibility of the evolution has been investigated by switching the electric field between 0 and 7 kV/mm for a number of cycles. As shown in the inset of Figure 4a, the Ti-O band of the BNT6BT ceramic cannot completely restore to the original shape after the first cycle of electric fields. The shoulder at ~300 cm^{-1} could be still observed, which, however, becomes diminished in subsequent cycles of electric fields. This demonstrates that, in agreement with the previous works, the tetragonal-to-rhombohedral phase transition is essentially irreversible. On the other hand, the increase in bandwidth for the Eu-BNT6BT ceramic (in the inset of Figure 4b) vanishes each time when the electric field is removed, demonstrating a high degree of reversibility. Namely, rather than a long-range stable ferroelectric state, the electric field induces a possible change from a globally pseudocubic symmetry with P4bm dominant PNRs to R3c PNRs state.[41,47,49] Although further investigation is needed for understanding the reversible evolution, it should be strongly related to the ergodic relaxor features of the ceramic.

The reversible features of the Eu-BNT6BT ceramic have also been examined using in-situ X-ray diffraction analysis, giving the results shown in Figure 5a. Probably due to the diminutive size of the ordered ferroelectric domains, no splitting of the three characteristic diffraction peaks {110}pc, {111}pc and {200}pc under high electric fields is observed for revealing the symmetries. The cubic-like lattices may also be the cause for the observed singlet diffraction peaks. On the other hand, all the characteristic diffraction peaks exhibit a shift to lower angles, by 0.15 - 0.2°, under a strong electric field of 7 kV/mm. This should be attributed to the lattice expansion induced by the electric field after the alignment of PNRs and formation of ordered ferroelectric domains.
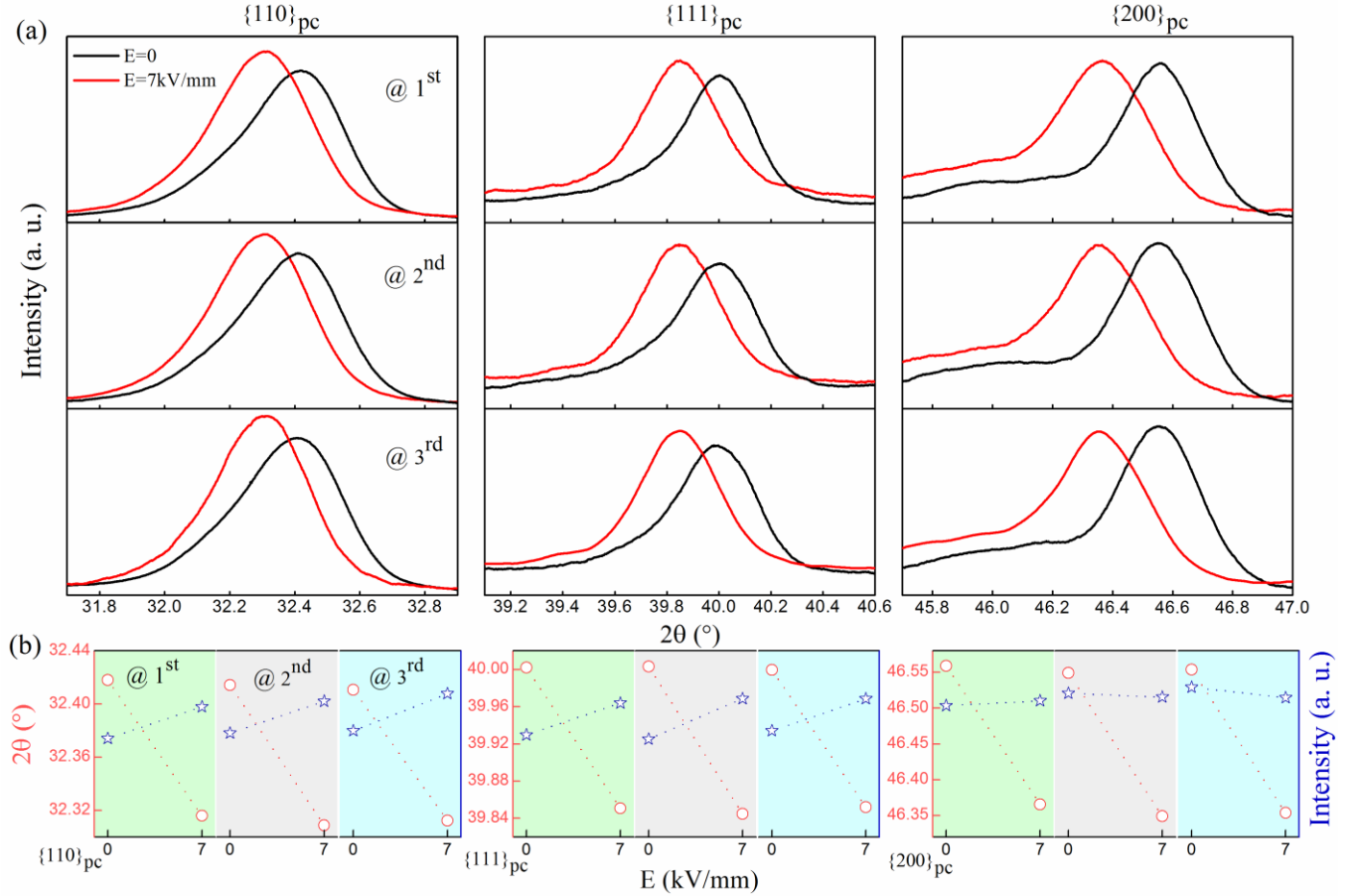
Figure 5 Fine XRD scanning of the Eu-BNT6BT ceramic: (a) patterns comparison when applying the off- and on-fields three times; (b) E field induced reversible angle (circle) and intensity (star) changes of the diffraction peaks are plotted accordingly.

Indeed, lattice distortion induced by the alignment because of the strong coupling with the matrix cannot be excluded. As also clearly shown in Figure 5b, the electric field-induced shifting of the peaks is highly reversible and can be fully repeated in subsequent cycles of electric fields.

3.4. In-situ PL Modification and Mechanism. Based on the above results, it is anticipated that the PL emissions of the Eu-BNT6BT ceramic can be effectively modulated by electric field via the induced reversible structural changes stemming from the ergodic relaxor features. Figure 6 first illustrates the effects of electric field on PL emissions of the ceramic measured under an excitation of 535 nm. Similar to other Eu-doped luminescent materials, the ceramic exhibits typical down-
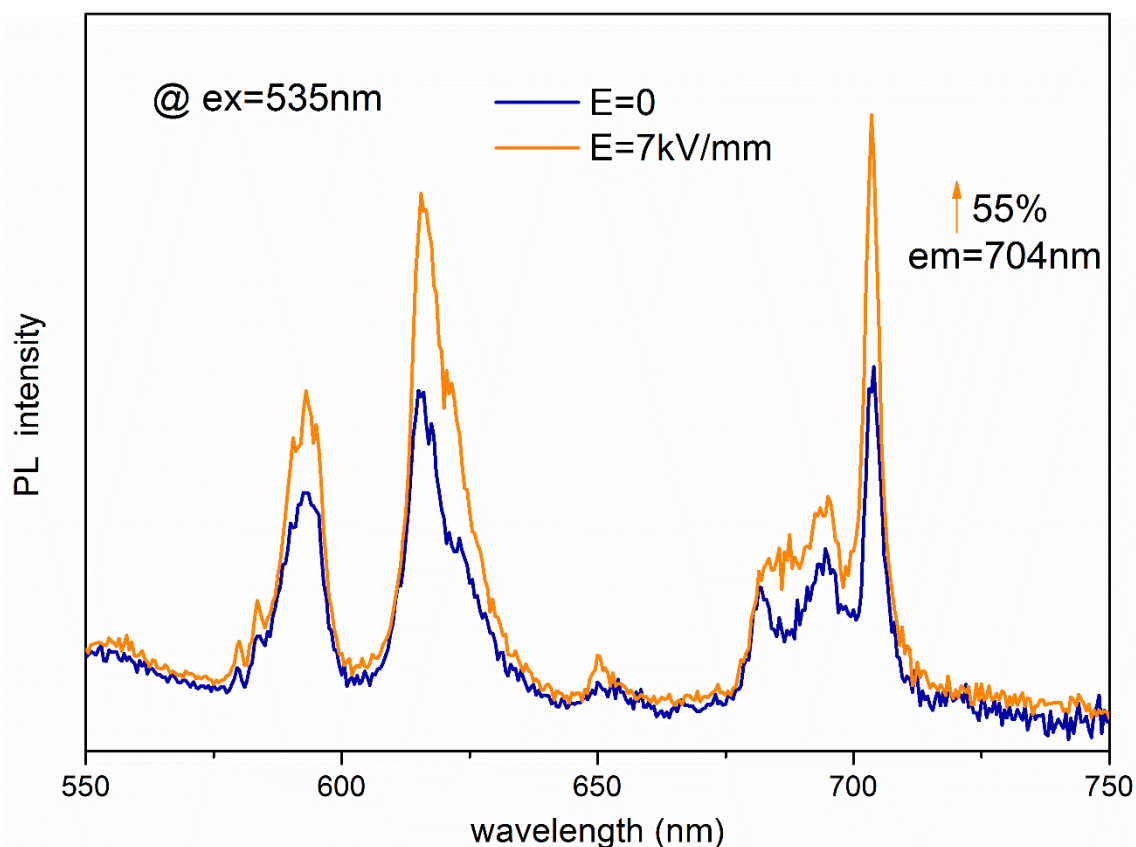
Figure 6 Effects of E field on the Photoluminescence emission spectrum of Eu-BNT6BT ceramic measured under an excitation of 535 nm.

----

conversion emissions at 590 nm, 615 nm and 704 nm, which are attributed to the transitions of Eu^{3+} ($^0D_5 \rightarrow {}^7F_1$, $^0D_5 \rightarrow {}^7F_2$ and $^0D_5 \rightarrow {}^7F_4$), respectively.[7,50-52] As clearly shown in Figure 6, the PL emissions are effectively enhanced by an electric field of 7 kV/mm, giving a maximum increase of 55% in PL intensity at 704 nm. An increase of 46% in the intensity of the excitation/absorption peak attributed to the $^7F_0 \rightarrow {}^5D_1$ transition has also been observed, by monitoring the emission at 704 nm, under the same electric field of 7 kV/mm (Figure S3). As no significant change in sample temperature has been observed using an infrared thermometer during the measurements, the thermal effects such as thermoluminescence and temperature-dependent PL could be excluded for the enhancements in both photoluminescence emissions and absorptions. Our results then affirm the capability of the structural symmetry reduction in enhancing photon absorptions and promoting

PL emissions, via the boost of uneven components of the local crystal field around the luminescent center, i.e., Eu^{3+}.[53-54] The uneven crystal field can mix opposite-parity states into the 4f configuration level and then increase the 4f-4f electric dipole transition probabilities of Eu^{3+}.[55] Under a strong electric field, the originally randomly oriented PNRs are aligned (by against the random fields) and ordered ferroelectric domains are formed, and then the lattices are distorted. These not only produce a large polarization and strain as shown in Figures 3a and 3b, but also reduce the structural symmetry and thus enhancing the PL emissions. Although a tetragonal-to-rhombohedral (P4bm to R3c symmetry) phase transition that usually occurs in BNT6BT ceramics cannot be confirmed in the Eu-BNT6BT ceramic in this work, the corresponding reduction in structural symmetry could also enhance the PL emissions.[56]
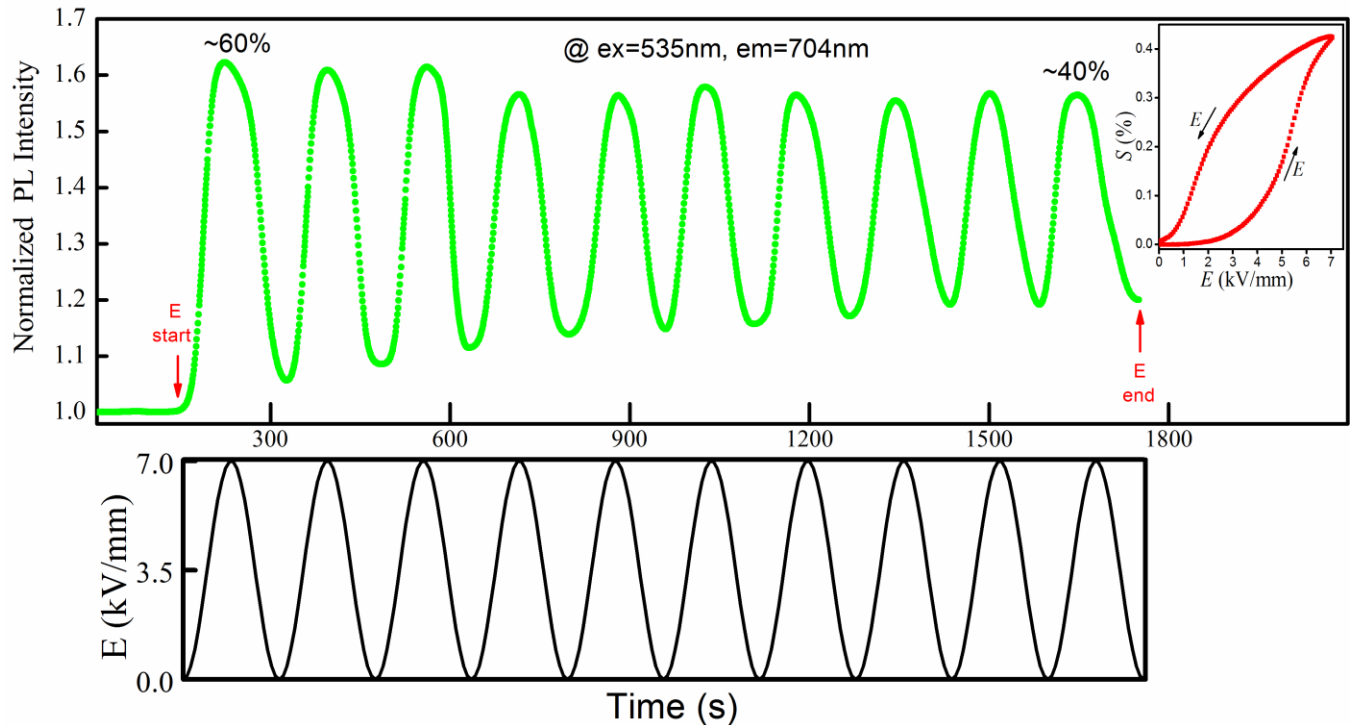

Figure 7 Large and tunable photoluminescence responses of Eu-BNT6BT relaxor subject to a biased ac E field varying sinusoidally between 0 and 7 kV/mm for cycles. The inset proposes the close relationship to the reversibly giant strain in Eu-BNT6BT with high ergodic state.

For investigating the reversibility of the E field-induced enhancement, the PL emission at 704 nm of the ceramic subject to a biased ac electric field varying sinusoidally between 0 and 7 kV/mm have been measured, giving the results shown in Figure 7. It can be clearly seen that as confirmed by the in-phase variations, the PL emission is modulated reversibly by the electric field. A large extent of modulation in PL intensity (~60%) is achieved in the first cycle of electric fields. However, it decreases gradually and saturates at ~40% in subsequent cycles of electric fields. This may be attributed to the gradual transition of some PNRs from ergodic relaxor state to non-ergodic relaxor state initiated probably by the weakening of the random fields during the alignments of PNRs. The decrease in reversibility may also indicate that some PNRs have undergone a transition from tetragonal phase to rhombohedral phase that has been shown to be irreversible in BNT6BT ceramics. On the other hand, the high reversibility of the real-time PL modulation should be mainly attributed to the high degree of ergodicity of the ceramic as confirmed above based on the dielectric/Raman/XRD studies as well as the P-E and S-E loops. Particularly, it is proposed that the origin of the tunable PL behavior is closely related to the large reversible strain in Eu-BNT6BT with a high ergodic state, as shown in the inset of Figure 7. As outlined earlier, the lattice distortion resulted from the evolution between dynamic PNRs and metastable ferroelectric state engenders a giant and reversal strain, which consequently affects the local crystal field around Eu^{3+} and thus modifies the emission performance.

4. CONCLUSION

We present a facile strategy for in-situ modulating photoluminescence (PL) emissions of Eu-BNT6BT ergodic relaxors continuously and reversibly using an external field at room temperature. Our results reveal that, due to the enhancement of random and weakly correlated PNRs, the electric field-induced ferroelectric state can restore to the original ergodic relaxor state after the

field removal, resulting in a reversible and large strain (~ 0.43% at 7 kV/mm). In-situ Raman and XRD results further confirm the ergodic relaxor nature at room temperature, both revealing a reversible feature of lattice distortion and crystal deformation resulted from the electric field-induced transformation between the dynamic PNRs and unstable ferroelectric state. Hence, PL of the Eu-BNT6BT relaxor can be manipulated by an electric field to a large extent of ~ 40% in a reversible fashion, attributed to tailoring the local crystal field around rare-earth ions. Not limited to the present work, these findings would stimulate next steps for realizing color tuning in rare-earth doped ergodic relaxors, also expand to other soft ferroelectrics in ergodic state, for high repeatability and flexible use of PL tuning at ambient temperature.

ASSOCIATED CONTENT

Supporting Information

Figure S1 Temperature dependences of dielectric constant (ε_r) and dielectric loss (tan δ) for the (a) un-poled and (b) poled pure BNT6BT ceramic; **Figure S2** Raman comparison of the samples without and with 1%Eu modification plotted in (a) raw and (b) normalized curves; **Figure S3** Photoluminescence excitation (PLE) spectra of Eu-BNT6BT sample in absence and presence of in-situ E-field under an emission of 704 nm.

AUTHOR INFORMATION

Corresponding Author

*Correspondence and requests for materials should be addressed to K.W.K. (email: apkwkwok@polyu.edu.hk). Fax: (852) 2333 7629. Tel.: (852) 53404890.

Author Contributions

Hailing Sun performed the experiments, analyzed the data and wrote the manuscript. Xiao Wu and Deng Feng Peng provided instructions for the experiments and analysis. K.W. Kwok advised on the in-situ electric-field controlling of tunable PL in current study, contributed to the discussion and interpretation of the results as well as revision on the manuscript.

Notes

The authors declare no competing financial interest.

REFERENCES

(1) De Greve, K.; Yu, L.; McMahon, P. L.; Pelc, J. S.; Natarajan, C. M.; Kim, N. Y.; Abe, E.; Maier, S.; Schneider, C.; Kamp, M.; Hofling, S.; Hadfield, R. H.; Forchel, A.; Fejer, M. M.; Yamamoto, Y. Quantum-Dot Spin-Photon Entanglement via Frequency Downconversion to Telecom Wavelength. *Nature* **2012,** 491, 421-425.

(2) Wang, F.; Han, Y.; Lim, C. S.; Lu, Y.; Wang, J.; Xu, J.; Chen, H.; Zhang, C.; Hong, M.; Liu, X. Simultaneous Phase and Size Control of Upconversion Nanocrystals Through Lanthanide Doping. *Nature* **2010,** 463, 1061-1065.

(3) Zhang, Q., Zheng, X., Sun, H., Li, W., Wang, X., Hao, X., An, S. Dual-Mode Luminescence Modulation upon Visible-Light-Driven Photochromism with High Contrast for Inorganic Luminescence Ferroelectrics. *ACS Appl. Mater. Interfaces* **2016,** 8, 4789-4794.

(4) Hao, J.; Zhang, Y.; Wei, X. Electric-Induced Enhancement and Modulation of Upconversion Photoluminescence in Epitaxial $BaTiO_3$:Yb/Er Thin Films. *Angew. Chem.* **2011,** 123, 7008-7012.

(5) Zhang, Q., Sun, H., Wang, X., Hao, X., An, S. Reversible Luminescence Modulation upon Photochromic Reactions in Rare-Earth Doped Ferroelectric Oxides by in Situ Photoluminescence Spectroscopy. *ACS Appl. Mater. Interfaces* **2015,** 7, 25289-25297.

(6) Zhang, Q., Zhang, Y., Sun, H., Geng, W., Wang, X., Hao, X., An, S. Tunable luminescence contrast of $Na_{0.5}Bi_{4.5}Ti_4O_{15}$: Re (Re= Sm, Pr, Er) photochromics by controlling the excitation energy of luminescent centers. *ACS Appl. Mater. Interfaces* **2016,** 8, 34581-34589.

(7) Khatua, D. K.; Kalaskar, A.; Ranjan, R. Tuning Photoluminescence Response by Electric Field in Electrically Soft Ferroelectrics. *Phys. Rev. Lett.* **2016,** 116, 117601.

(8) Yao, Q.; Wang, F.; Xu, F.; Leung, C. M.; Wang, T.; Tang, Y.; Ye, X.; Xie, Y.; Sun, D.; Shi, W. Electric Field-Induced Giant Strain and Photoluminescence-Enhancement Effect in Rare-Earth Modified Lead-Free Piezoelectric Ceramics. *ACS Appl. Mater. Interfaces* **2015,** 7, 5066-5075.

(9) Zhang, Q.; Sun, H.; Zhang, Y.; Ihlefeld, J. Polarization-Induced Photoluminescence Quenching in $(Ba_{0.7}Ca_{0.3}TiO_3)$-$(BaZr_{0.2}Ti_{0.8}O_3)$:Pr Ceramics. *J. Am. Ceram. Soc.* **2014,** 97, 868-873.

(10) Sun, H. L.; Wu, X.; Chung, T. H.; Kwok, K. In-situ Electric Field-Induced Modulation of Photoluminescence in Pr-doped $Ba_{0.85}Ca_{0.15}Ti_{0.90}Zr_{0.10}O_3$ Lead-Free Ceramics. *Sci. Rep.* **2016,** 6, 28677.

(11) Weyland, F.; Acosta, M.; Koruza, J.; Breckner, P.; Rödel, J.; Novak, N. Criticality: Concept to Enhance the Piezoelectric and Electrocaloric Properties of Ferroelectrics. *Adv. Funct. Mater.* **2016,** 26, 7326-7333.

(12) Ang, C.; Yu, Z. High, Purely Electrostrictive Strain in Lead-Free Dielectrics. *Adv. Mater.*

2006, 18, 103-106.

(13) Hong, C.-H.; Kim, H.-P.; Choi, B.-Y.; Han, H.-S.; Son, J. S.; Ahn, C. W.; Jo, W. Lead-Free Piezoceramics – Where to Move On? *J. Materiomics* **2016,** 2, 1-24.

(14) Dittmer, R.; Gobeljic, D.; Jo, W.; Shvartsman, V. V.; Lupascu, D. C.; Jones, J. L.; Rödel, J. Ergodicity Reflected in Macroscopic and Microscopic Field-Dependent Behavior of BNT-Based Relaxors. *J. Appl. Phys.* **2014,** 115, 084111.

(15) Jo, W.; Dittmer, R.; Acosta, M.; Zang, J.; Groh, C.; Sapper, E.; Wang, K.; Rödel, J. Giant Electric-Field-Induced Strains in Lead-Free Ceramics for Actuator Applications–Status and Perspective. *J. Electroceram.* **2012,** 29, 71-93.

(16) Dittmer, R. Lead-Free Piezoceramics–Ergodic and Nonergodic Relaxor Ferroelectrics Based on Bismuth Sodium Titanate; Technische Universität, Germany, **2013**.

(17) Groszewicz, P. B.; Breitzke, H.; Dittmer, R.; Sapper, E.; Jo, W.; Buntkowsky, G.; Rödel, J. Nanoscale Phase Quantification in Lead-Free $(Bi_{1/2}Na_{1/2})TiO_3$-$BaTiO_3$ relaxor Ferroelectrics by Means of ^{23}Na NMR. *Phys. Rev. B* **2014**, 90, 220104.

(18) Gobeljic, D.; Dittmer, R.; Rödel, J.; Shvartsman, V. V.; Lupascu, D. C. Macroscopic and Nanoscopic Polarization Relaxation Kinetics in Lead-Free Relaxors $Bi_{1/2}Na_{1/2}TiO_3$-$Bi_{1/2}K_{1/2}TiO_3$-$BiZn_{1/2}Ti_{1/2}O_3$. *J. Am. Ceram. Soc.* **2014**, 97, 3904-3912.

(19) Xu, C.; Lin, D.; Kwok, K. W. Structure, Electrical Properties and Depolarization Temperature of $(Bi_{0.5}Na_{0.5})TiO_3$-$BaTiO_3$ Lead-Free Piezoelectric Ceramics. *Solid State Sci.* **2008,** 10, 934-940.

(20) Simons, H.; Daniels, J. E.; Glaum, J.; Studer, A. J.; Jones, J. L.; Hoffman, M. Origin of Large Recoverable Strain in $0.94(Bi_{0.5}Na_{0.5})TiO_3$-$0.06BaTiO_3$ Near the Ferroelectric-Relaxor Transition. *Appl. Phys. Lett.* **2013,** 102, 062902.

(21) Jo, W.; Granzow, T.; Aulbach, E.; Rödel, J.; Damjanovic, D. Origin of the Large Strain Response in $(K_{0.5}Na_{0.5})NbO_3$-Modified $(Bi_{0.5}Na_{0.5})TiO_3$-$BaTiO_3$ Lead-Free Piezoceramics. *J. Appl. Phys.* **2009,** 105, 094102.

(22) Hiruma, Y.; Nagata, H.; Takenaka, T. Phase Diagrams and Electrical Properties of $(Bi_{1/2}Na_{1/2})TiO_3$-Based Solid Solutions. *J. Appl. Phys.* **2008,** 104, 124106.

(23) Wang, K.; Hussain, A.; Jo, W.; Rödel, J.; Viehland, D. D. Temperature-Dependent Properties of $(Bi_{1/2}Na_{1/2})TiO_3$-$(Bi_{1/2}K_{1/2})TiO_3$-$SrTiO_3$ Lead-Free Piezoceramics. *J. Am. Ceram. Soc.* **2012,** 95, 2241-2247.

(24) Xu, Q.; Chen, M.; Chen, W.; Liu, H. X.; Kim, B. H.; Ahn, B. K. Effect of Ln_2O_3 (Ln= La, Pr, Eu, Gd) addition on structure and electrical properties of $(Na_{0.5}Bi_{0.5})_{0.93}Ba_{0.05}TiO_3$ ceramics. *J. Alloys Compd.* **2008,** 463, 275-281.

(25) Hao, J.; Xu, Z.; Chu, R.; Li, W.; Fu, P.; Du, J.; Li, G. Large electrostrictive effect and strong photoluminescence in rare-earth modified lead-free $(Bi_{0.5}Na_{0.5})TiO_3$-based piezoelectric ceramics. Scripta Materialia, **2016,** 122, 10-13.

(26) Du, P.; Luo, L.; Li, W.; Zhang, Y.; Chen, H. Electrical and luminescence properties of Er-doped $Bi_{0.5}Na_{0.5}TiO_3$ ceramics. *Mater. Sci. Eng., B.* **2013,** 178, 1219-1223.

(27) Kholkin, A.; Morozovska, A.; Kiselev, D.; Bdikin, I.; Rodriguez, B.; Wu, P.; Bokov, A.; Ye, Z.-G.; Dkhil, B.; Chen, L.-Q.; Kosec, M.; Kalinin, S. V. Surface Domain Structures and Mesoscopic Phase Transition in Relaxor Ferroelectrics. *Adv. Funct. Mater.* **2011,** 21, 1977-1987.

(28) Malik, R. A.; Hussain, A.; Zaman, A.; Maqbool, A.; Rahman, J. U.; Song, T. K.; Kim, W.-J.; Kim, M.-H. Structure–Property Relationship in Lead-Free A- and B-Site Co-Doped $Bi_{0.5}(Na_{0.84}K_{0.16})_{0.5}TiO_3$-$SrTiO_3$ Incipient Piezoceramics. *RSC Adv.* **2015,** 5, 96953-96964.

(29) Garg, R.; Rao, B. N.; Senyshyn, A.; Krishna, P. S. R.; Ranjan, R. Lead-Free Piezoelectric

System (Bi$_{0.5}$Na$_{0.5}$)TiO$_3$-BaTiO$_3$: Equilibrium Structures and Irreversible Structural Transformations Driven by Electric Field and Mechanical Impact. *Phys. Rev. B* **2013,** 88, 014103.

 (30) Bai, W.; Chen, D.; Huang, Y.; Shen, B.; Zhai, J.; Ji, Z. Electromechanical Properties and Structure Evolution in BiAlO$_3$-Modified Bi$_{0.5}$Na$_{0.5}$TiO$_3$-BaTiO$_3$ Lead-Free Piezoceramics. *J. Alloys Compd.* **2016,** 667, 6-17.

 (31) Montero-Cabrera, M. E.; Pardo, L.; Garcia, A.; Fuentes-Montero, M. E.; Ballinas-Casarrubias, M. L.; Fuentes-Cobas, L. E. The global and Local Symmetries of Nanostructured Ferroelectric Relaxor 0.94(Bi$_{0.5}$Na$_{0.5}$)TiO$_3$-0.06BaTiO$_3$. *Ferroelectrics* **2014,** 469, 50-60.

 (32) Daniels, J. E.; Majkut, M.; Cao, Q.; Schmidt, S.; Wright, J.; Jo, W.; Oddershede, J. Heterogeneous Grain-Scale Response in Ferroic Polycrystals under Electric Field. *Sci. Rep.* **2016**, 6, 22820.

 (33) Ma, C.; Guo, H.; Beckman, S. P.; Tan, X. Creation and Destruction of Morphotropic Phase Boundaries through Electrical Poling: A Case Study of Lead-Free (Bi$_{1/2}$Na$_{1/2}$)TiO$_3$-BaTiO$_3$ Piezoelectrics. *Phys. Rev. Lett.* **2012**, 109 (10) 107602.

(34) Manley, M. E.; Lynn, J. W.; Abernathy, D. L.; Specht, E. D.; Delaire, O.; Bishop, A. R.; Budai, J. D. Phonon localization drives polar nanoregions in a relaxor ferroelectric. *Nat. Commun*. **2014**, 5, 3683.

 (35) Shvartsman, V. V.; Lupascu, D. C.; Green, D. J. Lead-Free Relaxor Ferroelectrics. *J. Am. Ceram. Soc.* **2012**, 95, 1-26.

(36) Egami, T.; Billinge, S. J. *Underneath the Bragg peaks: structural analysis of complex materials,* 2nd ed; Pergamon Publications: Oxford, **2012.**

 (37) Manley, M. E.; Abernathy, D. L.; Sahul, R.; Parshall, D. E.; Lynn, J. W.; Christianson, A. D.; Stonaha, P. J.; Specht, E. D.; Budai, J. D. Giant electromechanical coupling of relaxor

ferroelectrics controlled by polar nanoregion vibrations. Sci. Adv. **2016**, 2, e1501814.

(38) Jo, W.; Schaab, S.; Sapper, E.; Schmitt, L. A.; Kleebe, H.-J.; Bell, A. J.; Rödel, J. On the Phase Identity and Its Thermal Evolution of Lead Free $(Bi_{1/2}Na_{1/2})TiO_3$-6 mol%$BaTiO_3$. *J. Appl. Phys.* **2011**, 110, 074106.

(39) Shi, J.; Fan, H.; Liu, X.; Bell, A. J.; Roedel, J. Large Electrostrictive Strain in $(Bi_{0.5}Na_{0.5})TiO_3$-$BaTiO_3$-$(Sr_{0.7}Bi_{0.2})TiO_3$ Solid Solutions. *J. Am. Ceram. Soc.* **2014,** 97, 848-853.

(40) Jo, W.; Granzow, T.; Aulbach, E.; Rödel, J.; Damjanovic, D. Origin of the Large Strain Response in $(K_{0.5}Na_{0.5})NbO_3$-modified $(Bi_{0.5}Na_{0.5})TiO_3$-$BaTiO_3$ Lead-Free Piezoceramics. *J. Appl. Phys.* **2009**, 105, 094102.

(41) Anthoniappen, J.; Tu, C.-S.; Chen, P.-Y.; Chen, C.-S.; Idzerda, Y. U.; Chiu, S.-J. Raman Spectra and Structural Stability in B-Site Manganese Doped $(Bi_{0.5}Na_{0.5})_{0.925}Ba_{0.075}TiO_3$ Relaxor Ferroelectric Ceramics. *J. Eur. Ceram. Soc.* **2015**, 35, 3495-3506.

(42) Bai, W.; Chen, D.; Zheng, P.; Shen, B.; Zhai, J.; Ji, Z. Composition- and Temperature-Driven Phase Transition Characteristics and Associated Electromechanical Properties in $Bi_{0.5}Na_{0.5}TiO_3$-based Lead-Free Ceramics. *Dalton Trans.* **2016**, 45, 8573-8586.

(43) Hao, J.; Shen, B.; Zhai, J.; Liu, C.; Li, X.; Gao, X. Switching of Morphotropic Phase Boundary and Large Strain Response in Lead-Free Ternary $(Bi_{0.5}Na_{0.5})TiO_3$-$(K_{0.5}Bi_{0.5})TiO_3$-$(K_{0.5}Na_{0.5})NbO_3$ System. *J. Appl. Phys.* **2013,** 113, 114106.

(44) Aksel, E.; Forrester, J. S.; Kowalski, B.; Deluca, M.; Damjanovic, D.; Jones, J. L. Structure and properties of Fe-modified $Na_{0.5}Bi_{0.5}TiO_3$ at ambient and elevated temperature. *Phys. Rev. B* **2012,** 85, 024121.

(45) Suchanicz, J.; Jankowska-Sumara, I.; Kruzina, T. V. Raman and Infrared Spectroscopy of $Na_{0.5}Bi_{0.5}TiO_3$-$BaTiO_3$ Ceramics. *J. Electroceram.* **2011**, 27, 45-50.

(46) Hinterstein, M.; Schmitt, L. A.; Hoelzel, M.; Jo, W.; Rödel, J.; Kleebe, H. J.; Hoffman, M. Cyclic Electric Field Response of Morphotropic $Bi_{1/2}Na_{1/2}TiO_3$-$BaTiO_3$ Piezoceramics. *Appl. Phys. Lett.* **2015**, 106, 222904.

(47) Hao, J.; Bai, W.; Li, W.; Shen, B.; Zhai, J. Phase Transitions, Relaxor Behavior, and Large Strain Response in $LiNbO_3$-Modified $Bi_{0.5}(Na_{0.80}K_{0.20})_{0.5}TiO_3$ Lead-Free Piezoceramics. *J. Appl. Phys.* **2013,** 114, 044103.

(48) Shi, J.; Fan, H.; Liu, X.; Li, Q. Giant Strain Response and Structure Evolution in $(Bi_{0.5}Na_{0.5})_{0.945-x}(Bi_{0.2}Sr_{0.7}Na_{0.1})_x$-$Ba_{0.055}TiO_3$ Ceramics. *J. Eur. Ceram. Soc.* **2014,** 34, 3675-3683.

(49) Jaita, P.; Watcharapasorn, A.; Kumar, N.; Jiansirisomboon, S.; Cann, D. P. Lead- Free $(Bi_{0.70}Sr_{0.30})TiO_3$-Modified $Bi_{0.5}(Na_{0.80}K_{0.20})_{0.5}TiO_3$ Ceramics with Large Electric Field–Induced Strains. *J. Am. Ceram. Soc.* **2016,** 99, 1615-1624.

(50) Gong, C.; Li, Q.; Liu, R.; Hou, Y.; Wang, J.; Dong, X.; Liu, B.; Tan, X.; Liu, J.; Yang, K.; Zou, B.; Cui, T.; Liu, B. Structural Phase Transition and Photoluminescence Properties of YF_3:Eu^{3+} Nanocrystals under High Pressure. *J. Phys. Chem. C* **2014,** 118, 22739-22745.

(51) Kalaskar, A.; Rao, B. N.; Thomas, T.; Ranjan, R. Influence of Electric Field on the Eu^{+3} Photolumiscence in Lead-Free Ferroelectric $Na_{1/2}Bi_{1/2}TiO_3$. *arXiv preprint arXiv:*1507.05288 **2015**.

(52) Tao, F.; Wang, Z.; Yao, L.; Cai, W.; Li, X. Synthesis and Photoluminescence Properties of Truncated Octahedral Eu-Doped YF_3 Submicrocrystals or Nanocrystals. *J. Phys. Chem. C* **2007,** 111, 3241-3245.

(53) Ofelt, G. S. Intensities of Crystal Spectra of Rare-Earth Ions. *J. Chem. Phys.* **1962,** 37, 511-520.

(54) Judd, B. R. Optical Absorption Intensities of Rare-Earth Ions. *Phys. Rev.* **1962,** 127, 750-761.

(55) Wang, F.; Liu, X. Recent Advances in the Chemistry of Lanthanide-Doped Upconversion Nanocrystals. *Chem. Soc. Rev.* **2009,** 38, 976-89.

(56) Simons, H.; Daniels, J.; Jo, W.; Dittmer, R.; Studer, A.; Avdeev, M.; Rödel, J.; Hoffman, M. Electric-Field-Induced Strain Mechanisms in Lead-Free 94%$(Bi_{1/2}Na_{1/2})TiO_3$-6%$BaTiO_3$. *Appl. Phys. Lett.* **2011**, 98, 082901.

Table of Contents graphic